Pertanika J. Sci. & Technol. 21 (2): 459 - 472 (2013)

SCIENCE & TECHNOLOGY

Journal homepage: http://www.pertanika.upm.edu.my/

Electrical Conductivity of Anionic Surfactant-Doped Polypyrrole Nanoparticles Prepared via Emulsion Polymerization

Ghalib, H.[1,2], Abdullah, I.[1] and Daik, R.[1,2]*

[1]School of Chemical Sciences and Food Technology, Faculty of Science and Technology, Universiti Kebangsaan Malaysia, 43600 Bangi, Selangor, Malaysia
[2]Polymer Research Center (PORCE), Faculty of Science and Technology, Universiti Kebangsaan Malaysia, 43600 Bangi, Selangor, Malaysia

ABSTRACT

Conducting polypyrrole (PPy) nanoparticles were synthesized by chemical oxidative polymerization of pyrrole in aqueous solution containing ferric sulfate ($Fe_2(SO_4)_3$), anionic surfactants (sodium dodecylbenzene-sulfonate (NaDBS) or sodium dodecyl sulfate (SDS)), 1-pentanol as the oxidant, dopant and co-emulsifier, respectively. The polymerization was carried out at 0 ºC and 25 ºC. Fourier transform infrared spectroscopy (FTIR) and elemental analysis indicated that anionic surfactants were successfully incorporated into the PPy backbone. Incorporation of anionic surfactants caused enhanced electrical conductivity, increased yield, decreased the size of particles as well as improved the thermal stability of the resultant PPy. The presence of anionic surfactant seems to inhibit undesirable side reactions so as to improve the regularity of the PPy backbone. Globular PPy particles were obtained with diameter ranged from 40 to 118 nm as revealed by field emission scanning electron microscopy (FE-SEM) and conductivity of 7.89×10^{-4} –2.35×10^{-2} S cm^{-1}, as measured using impedance analyzer. It was found that polymerization at low temperature (0 ºC) produced PPy particles with smaller size and higher conductivity. The sodium dodecyl sulfate-doped PPy (SDS-doped PPy) exhibited higher conductivity than that of the sodium dodecylbenzenesulfonate-doped PPy (NaDBS-doped PPy), due to the bulkiness of NaDBS as compared to SDS.

Keywords: Polymer nanoparticle, conducting polymer, conjugated polymer, emulsion polymerization

INTRODUCTION

Over the last few decades, conducting polymers have attracted much attention because of their potential application in production of a variety of products such as electrodes for rechargeable batteries (Veeraraghavan *et al.,* 2002), actuators (Pyo *et*

Article history:
Received: 2 August 2011
Accepted: 2 July 2012

E-mail addresses:
h_ghalib1976@yahoo.com (Ghalib, H.),
dia@ukm.my (Abdullah, I.),
rusli@ukm.my (Daik, R.)
*Corresponding Author

ISSN: 0128-7680

al., 2003), sensors (Ramanavicius *et al.,* 2006), and solid electrolytes for capacitors (Yamamoto *et al.,* 1999). Among these conducting polymers, polypyrole (PPy) attracted special attention because of their outstanding characteristics, for instance good electrical conductivity, ease of synthesis, environmental stability, and non-toxicity (Wang *et al.,* 2001). PPy can be easily prepared by either electrochemical method to produce PPy films (Pringle *et al.,* 2004) or chemical method to yield PPy powders (Abraham *et al.,* 2001). The chemical method is suitable for commercial mass production and may produce processable PPy since this method allows a greater degree of control over the molecular weight and structural feature of the resulting polymer as compared to the electrochemical method (Lee *et al.,* 1995; Lee *et al.,* 1997).

Recently, the synthesis of nanostructured conducting materials has become an important branch of material research. These materials are expected to possess unique chemical and physical properties due to their finite small size and accordingly to offer a wide range of applications in a variety of fields including chemistry, physics, biomedical sciences, microelectronics and material science (Feng *et al.,* 2000).

Emulsion polymerization allows the formation of polymer particles with diameter ranges from 10 nm to 100 nm. Usually, a number of emulsifiers, such as ionic surfactant (e.g., sodium dodecyl-benzene sulfonate (NaDBS)) together with short-chain alcohols are used in the reaction medium (Antony & Jayakannan 2009; Liu *et al.,* 2006). It has been reported that PPy nanoparticles obtained from emulsion polymerization were in the range of about 50 to 100 nm and 100 to 200 nm with the change in the concentration of surfactant (dodecyltrimethyl ammonium bromide (DTAB)) from 0.8 to 0.44 M (Wang *et al.,* 2005), respectively. Conducting PPy nanoparticles with diameter of 30–50 nm could also be prepared via emulsion polymerization with $FeCl_3$ as the oxidant (Yan *et al.,* 2000). It was found that, the emulsion polymerization produced higher yield of the resultant PPy as compared to the solution polymerization. PPy nanoparticles have been synthesized in the presence of different dopants including hydrochloric acid (HCl), p-toluene sulfonic acid (TSA), camphor sulfonic acid (CSA), and polystyrene sulfonic acid (PSSA). These doped PPy nanoparticles exhibited electrical conductivity in the range of 20×10^{-4} - 6×10^{-2} S cm^{-1} (Goel *et al.,* 2010).

Conductivity and environmental stability of doped PPy at room temperature were reported by (Kudoh 1996). Omastova´ *et al.* (2003) reported the synthesis of PPy using $Fe_2(SO_4)_3$ as the oxidant with different surfactants at 25 ºC. The effect of type of surfactant on stability, conductivity and morphology was studied. They suggested that the presence of anionic surfactant in polymerization mixture strongly influenced the morphology of chemically prepared PPy. However, to the best of our knowledge, the study on the synthesis of PPy nanoparticles with $Fe_2(SO_4)_3$ and anionic surfactants (NaDBS, SDS) at 0 ºC and 25 ºC has seldom been reported.

Thus the purpose of this study is to examine the effect of polymerization temperature and type of doping agent (NaDBS and SDS) on the morphology, electrical conductivity and thermal stability of the PPy nanoparticles synthesized by chemical oxidation.

MATERIALS AND METHODS

Materials

Pyrrole of 97% purity (Aldrich) was purified by leaching through a column of activated basic alumina and then stored at 4 ºC prior to use. The oxidant, ferric sulfate ($Fe_2(SO_4)_3$), was purchased from Riedel-De Haen Ag Seelze-Hannover. 1-Pentanol was obtained from BDH chemicals Ltd., Poole, England. Sodium dodecyl sulfate (SDS) and aluminum oxide were purchased from Merck while sodium dodecyl benzene sulphonate (NaDBS) was obtained from Aldrich. All chemicals were used as received. Deionized water was used in all experiments.

Preparation of PPy Nanoparticles

The typical experiment is described as follows. SDS (8.7 g) or NaDBS (10.5 g) was dissolved in deionized water (300 mL) and stirred vigorously at 0 ºC or 25 ºC. A mixture of pyrrole (2 mL) and 1-pentanol (4 mL) was added to this solution. After 1 h, a ferric sulfate aqueous solution (11.6 g of $Fe_2(SO_4)_3$ in 50 mL of deionized water) was introduced dropwise over a period of 2 h to the above solution. The reaction was allowed to proceed for 3 h. An excessive amount of methanol was then added to the mixture. The resultant precipitate of the doped PPy nanoparticles was filtered and washed several times with deionized water, methanol and acetone, successively. Finally, the product was dried for 7 h under vacuum at 60–70 ºC. For comparison purposes, PPy (undoped PPy) was also synthesized under similar conditions, but without using surfactant.

Characterization

The FTIR spectra of PPy nanoparticles were obtained via KBr pellets on a Perkin Elmer FT-IR system Spectrum GX. The spectra were recorded over the wavenumber range of 600–4000 cm^{-1}. The PPy contents were determined through elemental analysis using a CHNS Thermo Finnigan Eager 300 for EA 1112 elemental analyzer. The specimens used for conductivity measurement were in pellet form with diameter and thickness of 13 mm and 1.5 mm, respectively. The PPy samples were compressed using a load of 5 ton for 5 minutes. The obtained samples were analyzed by using a frequency response analyzer (Solatron Schlumberger 1260 HF). The impedance spectra were recorded over the frequency range of 1 Hz-10 MHz at room temperature.

Field emission scanning electron microscopy (FE-SEM) images were recorded with a SUPRA 55VP microscope (Zeiss, Germany). Thermal stability study was carried out using the thermogravimetry analyzer TGA/SDTA851.

RESULTS AND DISCUSSION

FTIR Spectroscopy

The FTIR spectra of various samples of PPy particles synthesized in this work are presented in Fig.1. The vibrational frequencies of the major infrared peaks and their assignment are summarized in Table 1. All the spectra displayed few strong bands in the 1600–600 cm^{-1} region

which are common characteristics of PPy (Chen & Xue 2010; Li *et al.,* 2007; Omastová *et al.,* 2003). The FTIR spectra of doped PPy nanoparticles in general showed spectral characteristics similar to those of undoped PPy, indicating that the doped PPy nanoparticles have similar chain structures to undoped counterpart.

The peak at 1698 cm^{-1} observed in the spectrum of undoped PPy (Fig.1a) can be attributed to the presence of the carbonyl group formed by nucleophilic attack of water during the preparation process (Liu *et al.,* 2009; Thiéblemont *et al.,* 1994; Zhong *et al.,* 2006). The peak at 1551 cm^{-1}, which corresponds to the C-C/C=C stretching vibrations in the pyrrole ring, was observed in the spectrum of undoped PPy. This corresponding peak, however, was red-shifted to lower wavenumbers; 1541, 1544, and 1545 cm^{-1}, in the spectra of the doped PPy nanoparticles (Fig.1b, Fig.1c, Fig.1d, and Fig.1e). It is known that the skeletal vibrations, involving the delocalized π-electrons, are affected by doping the polymer (Omastová *et al.,* 2004). The observed shift may be caused by the ionic interaction of anionic surfactant with polypyrrole. Likewise, the peak at 1475 cm^{-1} that is due to the C–N stretching vibration of undoped PPy was red-shifted to 1456 and 1459 cm^{-1} in the spectra of the doped PPy nanoparticles. On the other hand, the peak of the C–H or C-N in–plane deformation observed at around 1291 cm^{-1} in the spectrum of undoped PPy was blue-shifted to 1301, 1302, 1303, and 1307 cm^{-1} in the spectra of the doped PPy nanoparticles. Moreover, the breathing vibration of the pyrrole ring, located at 1192 cm^{-1} in the spectrum of undoped PPy, was shifted to 1167, 1167, 1170, and 1173 cm^{-1} in the spectra of the doped PPy nanoparticles. Furthermore, the expected peak of the S=O stretching vibration of SO_3^- at 1183 cm^{-1} (Dutta & De 2003; Varela *et al.,* 2003) could not be clearly observed due to overlapping with the pyrrole ring vibration at 1192 cm^{-1}.

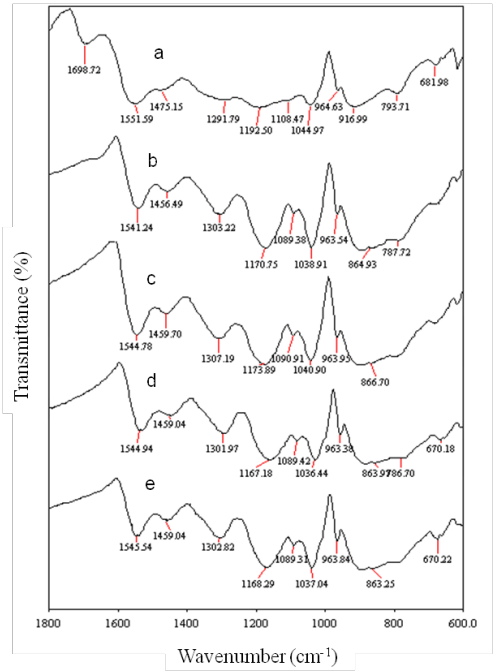

Fig.1: The FTIR spectra of (a) undoped PPy synthesized at 25ºC; SDS-doped PPy synthesized (b) at 0ºC (c) at 25 ºC; and NaDBS-doped PPy synthesized (d) at 0 ºC (e) at 25ºC

The peak at 1091 cm^{-1} corresponds to the mode of in-plane deformation vibration of the N^+H_2 which was formed in doped PPy nanoparticles chains by protonation (Omastová *et al.,* 2003). This particular peak was not observed in the spectrum of undoped PPy. The band of C–H and N-H in-plane deformation vibration which is usually located at 1044 cm^{-1} (Antony & Jayakannan 2009) in the spectrum of undoped PPy was observed at 1036, 1037, 1038, and 1040 cm^{-1} in the spectra of the doped PPy nanoparticles. The band observed at 964 cm^{-1} can be ascribed to the C-C out-of-plane ring deformation vibration and was located at the same wavenumber in the spectra of all samples. The band of C–H out-of-plane ring deformation observed at 793 cm^{-1} in the spectrum of undoped PPy was shifted to 784, 786, and 787 cm^{-1} in

TABLE 1
Major FTIR peaks and their assignments for undoped PPy and doped PPy nanoparticles

	Wavenumbers (cm^{-1})				
Peak assignments	PPy-SO_4	SDS-doped PPy at 0 ºC	SDS-doped PPy at 25 ºC	NaDBS-doped PPy at 0 ºC	NaDBS-doped PPy at 25ºC
1. The C-C/C=C stretching vibrations in pyrrole ring	1551	1541	1544	1544	1545
2. The C–N stretching vibration in the ring	1475	1456	1459	1459	1459
3. The peak of C–H or C-N in–plane deformation	1291	1303	1307	1301	1302
4. The breathing vibration of the pyrrole ring	1192	1170	1173	1167	1168
5. The mode of in-plane deformation vibration of the N^+H_2	-	1089	1090	1089	1089
6. The band of C–H and N-H in-plane deformation vibration	1044	1038	1040	1036	1037
7. The characteristic C-C out of plane ring deformation vibration	964	964	964	964	964
8. The band of C–H out of plane ring deformation	793	787	784	786	786
9. The peak of C-C out-of plane ring deformation or C–H rocking	681	670	670	670	670
10. The carbonyl group	1698	-	-	-	-
11. Methylene in PPy prepared from SDS	-	2917	2917	-	-
12. Methylene in PPy prepared from NaDBS	-	-	-	2851	2851

the spectra of the doped PPy nanoparticles. On the other hand, the peak of C-C out-of plane ring deformation or C–H rocking usually situated at 681 cm^{-1} (Omastova *et al.,* 1996) was shifted to around 670 cm^{-1}.

Morphology study

Fig.2 presents the FE-SEM micrographs of PPy nanoparticles prepared in this study. The FE-SEM micrograph of undoped PPy revealed the presence of globular structure with diameter of about 450-500 nm (Fig.2a).

The synthesis of PPy in the presence of NaDBS or SDS at 25 ºC produced nanoparticles of almost spherical shape with diameter ranged from 73 to 118 nm (Fig.2b and Fig.2d). This means that the addition of anionic surfactant to the polymerization mixture tremendously reduced the size of PPy nanoparticles. This finding is in good agreement with the previous reports (Antony & Jayakannan 2007, 2009; Jang 2006; Kwon *et al.,* 2008; Yang *et al.,* 2012). Fig.2b showed that the size of NaDBS-doped PPy nanoparticles prepared at 25 ºC was in the range of 73-107 nm while the size of the SDS-doped PPy nanoparticles ranged from 80 to 118 nm (Fig.2d).

On the other hand, the doped PPy synthesized at 0 ºC produced smaller nanoparticles (Fig.2c and Fig.2e) than those synthesized at 25 ºC (Fig.2b and Fig.2d). The NaDBS-doped PPy particles prepared at 0 ºC were in the range of 40-68 nm (Fig.2c) whereas the SDS-doped PPy ones were in the range of 47-83 nm (Fig.2e). These variations can be ascribed to the effect of temperature on the micelles, which consist of anionic surfactant and pyrrole monomer (Antony & Jayakannan 2009; Jang 2006; Kwon *et al.,* 2008; Yang *et al.,* 2012; Zhong *et al.,* 2006). At low temperature, mobility of the anionic surfactant is limited, leading to a decrease in the inner volume of micelles that encapsulate the monomer and the oxidant. Consequently, the reduced micelle volume results in reduced particle size (Wang *et al.,* 2005).

Elemental analysis

Table 2 shows the elemental composition, doping level, and mass recovery of all PPy samples prepared in this work. The high sulfur content in samples of doped PPy nanoparticles indicated the successful incorporation of anionic surfactants into the PPy backbone. This observation is in agreement with the previous works reported by other researchers, (Kudoh 1996; Lee *et al.,* 2000).

As shown in Table 2, the doping level of the doped PPy nanoparticles, which were calculated based on the elemental analysis results, was in the range of 21.8%–24.0%. These results indicate that, on the average, the doping level was about one dopant per five pyrrole units for both the NaDBS-doped PPy and the SDS-doped PPy nanoparticles synthesized at 0 ºC and at 25 ºC. These results also indicate that the synthesis of PPy with the presence of surfactant resulted in better mass recovery as compared to the one without surfactant. Likewise, the doped PPy nanoparticles prepared at 0 ºC showed higher mass recoveries than those prepared at 25 ºC. This is probably due to the fact that the growing sites of the polymer with free radicals are stabilized at low temperature (Lee *et al.,* 1997). Thus, at low temperature the propagation rate is greater than the initiation rate and consequently a higher mass recovery was obtained. On the other hand, at high temperature, the decomposition rate of the oxidant is high and may induce

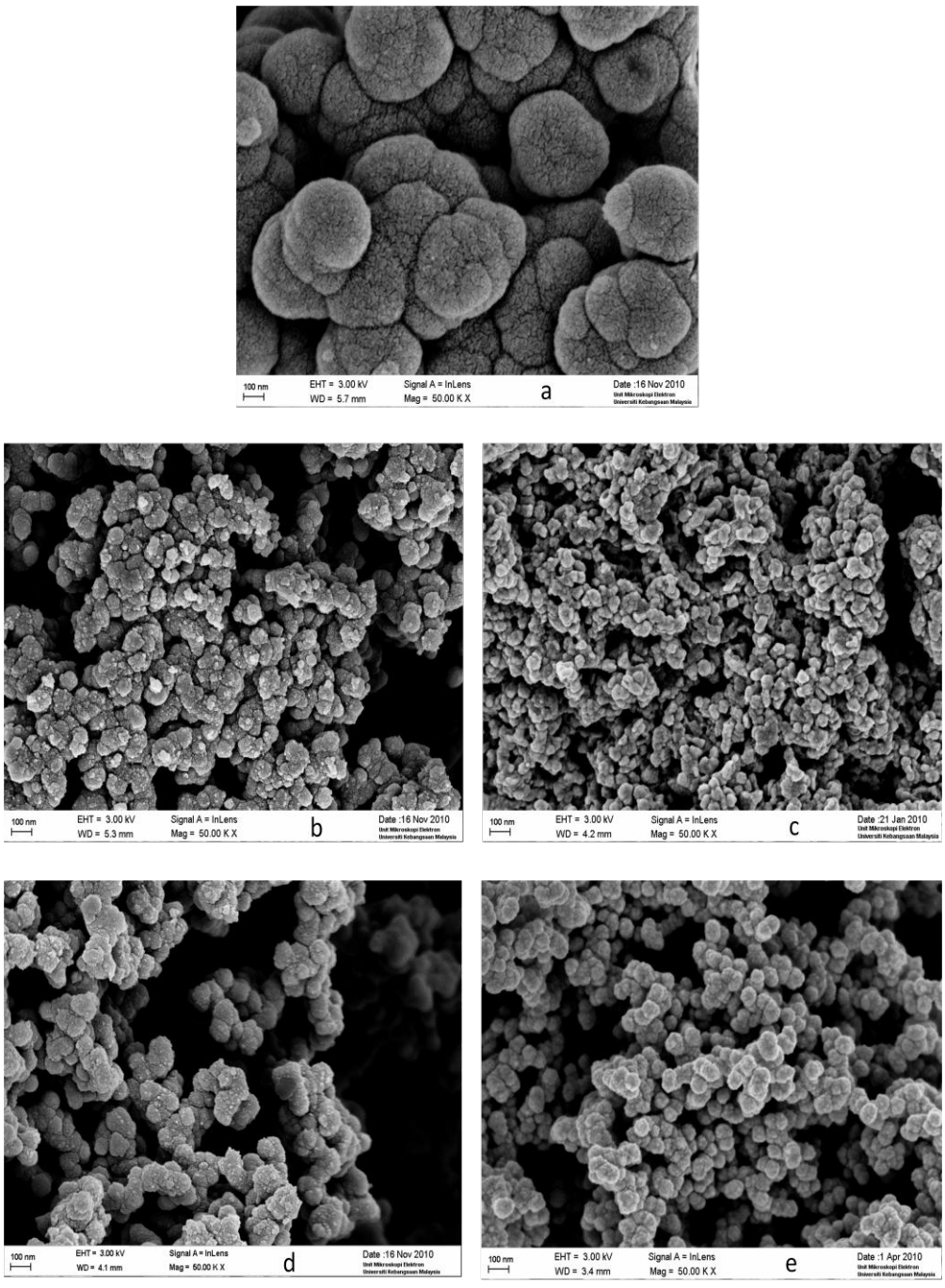

Fig.2: FE-SEM images of (a) undoped PPy synthesized at 25ºC; NaDBS-doped PPy synthesized (b) at 25ºC (c) at 0ºC; and SDS-doped PPy synthesized (d) at 25ºC (e) at 0 ºC (50,000 X)

high rate of chain termination of radical cations and conformation defects with branching or crosslinking of molecules (Lascelles *et al.,* 1998; Lee *et al.,* 1997), and ultimately, a low mass recovery will be obtained.

The NaDBS-doped PPy nanoparticles exhibited higher mass recovery than the SDS-doped PPy ones due to NaDBS being a bulky dopant as compared with the SDS. It has been commonly observed that the mass recovery increases with the bulkiness of the dopant (Abraham *et al.,* 2001; Akinyeye *et al.,* 2006; Song *et al.,* 2004).

TABLE 2
The elemental composition, doping level and mass recovery of undoped PPy and doped PPy nanoparticles

Polymers	Reaction temperature (°C)	Oxidant	N	C	H	S	S/N	Doping Level (%, ±1)	Mass Recovery (%)
Undoped PPy	25	$Fe_2(SO_4)_3$	13.34	45.95	2.89	1.41	0.11	04.8	21.20
NaDBS-doped PPy	0	$Fe_2(SO_4)_3$	10.27	54.99	6.54	5.68	0.55	24.0	45.71
NaDBS-doped PPy	25	$Fe_2(SO_4)_3$	10.29	54.02	6.14	5.31	0.52	22.8	36.84
SDS-doped PPy	0	$Fe_2(SO_4)_3$	10.10	58.37	6.46	5.59	0.51	22.2	36.88
SDS-doped PPy	25	$Fe_2(SO_4)_3$	11.06	58.58	6.49	5.51	0.50	21.8	26.82

Thermogravimetric analyses

The TGA and DTG thermograms of undoped PPy and the doped PPy nanoparticles are presented in Fig.3 and Fig.4. The initial degradation temperatures, the maximum degradation temperature and the residual weights at 600°C are listed in Table 3. The undoped PPy and the doped PPy nanoparticles have some adsorbed moisture, which is released around 100°C. The undoped PPy started to lose its weight at a relatively low temperature (148 °C) and the maximum degradation occurred at around 266 °C, while the residue at 600 ºC was 61%.

The thermal stability of doped PPy nanoparticles is dependent on the type of surfactant, the SDS-doped PPy nanoparticles started to degrade at 165 and 166 °C, whereas the NaDBS-doped PPy samples started to degrade at 230 °C. The maximum degradation of the SDS-doped PPy nanoparticles was observed at 275.6 °C and at 276.03 °C (Curves b and c in Fig.3 and Fig.4) whereas that of the NaDBS-doped PPy nanoparticles occurred at around 357 °C and 367 °C (Curves e and f in Fig.3 and Fig.4). These differences can be attributed to the lower degradation temperature of pure SDS (180-300 °C) as compared to pure NaDBS (400-500 °C) as illustrated by the curves a and g, respectively, in Fig.3 and Fig.4. This argument supports the inference drawn from our own results of elemental analysis and FTIR spectroscopy in which the anionic surfactant is incorporated as counterion into the PPy backbone (Dutta & De 2003).

The curves of NaDBS-doped PPy prepared at both 0 ºC and at 25 ºC indicated that the two samples exhibit a similar trend of weight loss. However, the NaDBS-doped PPy prepared at 0 ºC seemed to be slightly more thermally stable than the NaDBS-doped PPy prepared at 25 ºC. In addition, the SDS-doped PPy prepared at 0 ºC showed a slightly better thermal

stability as compared to the SDS-doped PPy prepared at 25 ºC. In all doped PPy samples, the residues at 600 ºC of doped PPy ranged from 51% to 58 %, thus indicating that the doped PPy nanoparticles do not completely degrade in nitrogen and that they can probably be carbonized to form graphitic forms (Yang *et al.,* 2010).

TABLE 3
Thermogravimetric data of undoped PPy and doped PPy nanoparticles

Sample	Reaction temperature (ºC)	Initial degradation temperature (ºC)	Maximum Degradation temperature (ºC)	Residue at 600 ºC (%)
Undoped PPy	25	148	266.16	61
NaDBS-doped PPy	0	230	367.20	53
NaDBS-doped PPy	25	230	357.01	51
SDS-doped PPy	0	166	276.03	58
SDS-doped PPy	25	165	275.63	51

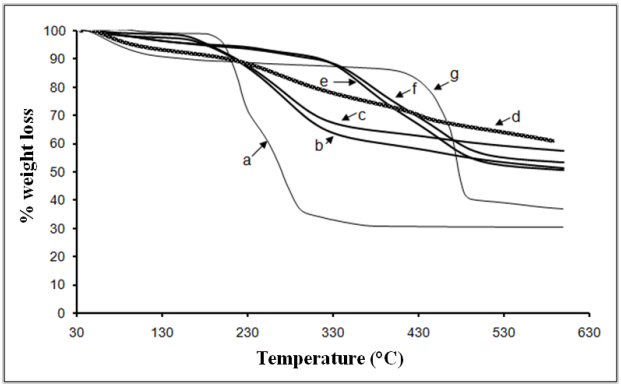

Fig.3: The TGA thermograms of (a) Neat SDS; SDS-doped PPy synthesized (b) at 25 ºC (c) at 0 ºC; (d) undoped PPy synthesized at 25ºC; NaDBS-doped PPy synthesized (e) at 25ºC (f) at 0ºC; and (g) Neat NaDBS

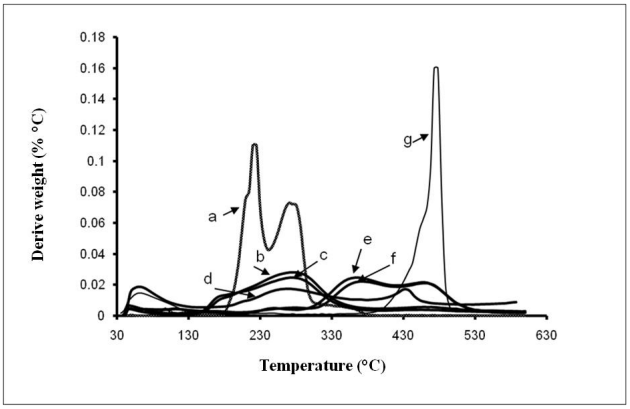

Fig.4: DTG thermograms of (a) Neat SDS, SDS-doped PPy synthesized (b) at 25 ºC (c) at 0 ºC (d) undoped PPy synthesized at 25 ºC, NaDBS-doped PPy synthesized (e) at 25 ºC (f) at 0 ºC and (g) Neat NaDBS

Electrical conductivity

The electrical conductivity of the PPy sample synthesized at 25 ºC without the presence of surfactant (undoped PPy) was 1.80×10^{-5} S cm^{-1} (Table 4), whereas the PPy sample synthesized in the presence of NaDBS or SDS at the same temperature showed higher electrical conductivity (7.89×10^{-4} - 2.80×10^{-3} S cm^{-1}).

In a typical polymerization, pyrrole rings are coupled through the α–α positions which create the main polymer chain. However, the α-β coupling also takes place, hence results in cross-linked PPy. In addition, some carbonyl and hydroxyl groups may also be present as a result of oxidation, especially in aqueous medium (Jang *et al.,* 2004). All these factors shorten the conjugation length of the PPy chain and reduce the mobility of the charge carriers, eventually the electrical conductivity. On the other hand, it has been reported that the presence of surfactant inhibited the formation of some carbonyl and hydroxyl groups or cross-linked PPy and thus the formation of relatively longer conjugation length with more regularity is possible. This will lead to a better mobility of charge carriers and subsequently increase the electrical conductivity (Omastová *et al.,* 2004). This argument is further supported by the FTIR results since carbonyl peak was observed in the spectrum of the undoped PPy at 1698 cm^{-1} (Fig.1a), whereas no similar peak in the spectrum of the doped PPy nanoparticles was observed. Furthermore, the main peaks of the undoped PPy (Fig.1a) were red-shifted to lower wavenumbers in the spectra of the doped PPy nanoparticles (Fig.1b, Fig.1c, Fig.1d and Fig.1e), consequently demonstrating the high electrical conductivity of these samples. This finding bears resemblance of the results reported earlier by Kwon *et al.* (2008) who reported that nanoparticles with high conductivity showed a red shift while those with low conductivity showed a blue one. The red shift of the main peaks indicated to the well conjugation and few contortion of PPy nanoparticles chains (Fang *et al.,* 2003), which facilitate the mobility of the charge carriers and hence, increase the electrical conductivity.

The SDS-doped PPy nanoparticles showed the highest electrical conductivities (2.80×10^{-3}-2.35×10^{-2} S cm^{-1}), while the NaDBS-doped PPy nanoparticles exhibited the lowest conductivities (7.89×10^{-4} to 1.34×10^{-3} S cm^{-1}). It is known that the electrical conductivity of conducting polymers is due to transport of charge carriers along the polymer chain as well as the transport of charge carriers from one chain to others (Liu & Wan 2001). The presence of bulky anion like NaDBS perturbs the arrangement of PPy chains, which results in increase in the intermolecular distance and hence, causes a partial restraint in the interchain hopping transport of charge carriers, which accordingly reduces the electrical conductivity (Kudoh *et al.,* 1998).

The doped PPy nanoparticles prepared at 0 ºC produced a polymer with higher electrical conductivity than those prepared at 25 ºC. This can be attributed to the regularity of the PPy backbone being improved because side reactions were inhibited. Besides, bonding between the α positions in the Py units during the polymerization at 0 ºC profoundly elevates the conjugation and subsequently the conductivity (Lascelles *et al.,* 1998). This explanation is additionally supported by the increased doping level (Table 2), uniform and small particles sizes (40–83 nm), and the highest electrical conductivity (1.34×10^{-3}-2.35×10^{-2} S cm^{-1}) attained at this temperature (Fig.2c and Fig.2e).

TABLE 4
The electrical conductivity of the undoped PPy and various doped PPy nanoparticles

Polymer	Reaction temperature (°C)	Electrical Conductivity(S cm^{-1})
Undoped PPy	25	1.80×10^{-5}
NaDBS-doped PPy	0	1.34×10^{-3}
NaDBS-doped PPy	25	7.89×10^{-4}
SDS-doped PPy	0	2.35×10^{-2}
SDS-doped PPy	25	2.80×10^{-3}

CONCLUSION

Conducting doped PPy nanoparticles were chemically synthesized using NaDBS and SDS as dopants, 1-pentanol as a co-emulsifier, and $Fe_2(SO_4)_3$ as an oxidant at 0 ºC and 25 ºC. The presence of NaDBS or SDS in the polymerization mixture affected the properties of the chemically-prepared, doped PPy nanoparticles (enhanced electrical conductivity, increased yield, decreased the size of particles as well as improved the thermal stability of the resultant PPy) due to bonding of the anionic part of the surfactant molecules with the PPy chains. The results of elemental analysis and FTIR spectroscopy demonstrated that, the surfactant was incorporated into the PPy structure. This result is supported by the TGA and DTG results. The mass recovery of the doped PPy nanoparticles ranged from 26.82% to 45.71% whereas the doping levels, which were calculated based on the elemental analysis data, were in the range 21.84%–24.02%. Globular PPy nanoparticles with diameters of 40–118 nm and conductivities in the range of 7.89×10^{-4}–2.35×10^{-2} S cm^{-1} were produced. The doped PPy nanoparticles prepared at 0 ºC produced a polymer with higher electrical conductivity than that prepared at 25 ºC. While the SDS-doped PPy nanoparticle samples showed the highest electrical conductivity (2.80×10^{-3}-2.35×10^{-2} S cm^{-1}), the NaDBS-doped PPy nanoparticle samples exhibited the lowest conductivities; 7.89×10^{-4} to 1.34×10^{-3} S cm^{-1}. This is due to the bulkiness of NaDBS as compared to SDS.

REFERENCES

Abraham, D., Jyotsna, T. S., & Subramanyam, S. V. (2001). Polymerization of pyrrole and processing of the resulting polypyrrole as blends with plasticised PVC. *Journal of Applied Polymer Science, 81*(6), 1544-154 8.

Akinyeye, R., Michira, I., Sekota, M., Al-Ahmed, A., Baker, P., & Iwuoha, E. (2006). Electrochemical Interrogation and Sensor Applications of Nanostructured Polypyrroles. *Electroanalysis, 18*(24), 2441-2450.

Antony, M. J., & Jayakannan, M. (2007). Amphiphilic Azobenzenesulfonic Acid Anionic Surfactant for Water-Soluble, Ordered, and Luminescent Polypyrrole Nanospheres. *The Journal of Physical Chemistry B, 111*(44), 12772-12780.

Antony, M. J., & Jayakannan, M. (2009). Self-assembled anionic micellar template for polypyrrole, polyaniline, and their random copolymer nanomaterials. *Journal of Polymer Science Part B: Polymer Physics, 47*(8), 830-846.

Chen, W., & Xue, G. (2010). Formation of conducting polymer nanostructures with the help of surfactant crystallite templates. *Frontiers of Materials Science in China, 4*(2), 152-157.

Dutta, P. & De, S. K. (2003). Electrical properties of polypyrrole doped with [beta]-naphthalenesulfonicacid and polypyrrole-polymethyl methacrylate blends. *Synthetic Metals, 139*(2), 201-206.

Fang, Q., Xu, W., Lei, H., Xue, G., Chen, H., Xu, C., Jia, C., & Zhang, D. (2003). Synthesis, structure, and conductivity of molecular conductor (PyEt)[Ni(dmit)$_2$]$_2$. *Science in China Series B: Chemistry*, *46*(6), 595-604.

Feng, Y., Gi, X., & Mingshi, Z. (2000). Preparation of electrically conducting polypyrrole in oil/water microemulsion. *Journal of Applied Polymer Science, 77*(1), 135-140.

Goel, S., Mazumdar, N. A., & Gupta, A. (2010). Synthesis and characterization of polypyrrole nanofibers with different dopants. *Polymers for Advanced Technologies, 21*(3), 205-210.

Jang, J. (2006). Conducting Polymer Nanomaterials and Their Applications. In (Eds.). *Emissive Materials Nanomaterials*. Berlin: Springer-Verlag Berlin.

Jang, J., Li, X. L., & Oh, J. H. (2004). Facile fabrication of polymer and carbon nanocapsules using polypyrrole core/shell nanomaterials. *Chemical Communications*, *7*, 794-795.

Kudoh, Y. (1996). Properties of polypyrrole prepared by chemical polymerization using aqueous solution containing $Fe_2(SO_4)_3$ and anionic surfactant. *Synthetic Metals, 79*(1), 17-22.

Kudoh, Y., Akami, K., & Matsuya, Y. (1998). Properties of chemically prepared polypyrrole with an aqueous solution containing $Fe_2(SO_4)_3$, a sulfonic surfactant and a phenol derivative. *Synthetic Metals*, *95*(3), 191-196.

Kwon, W. J., Suh, D. H., Chin, B. D., & Yu, J. W. (2008). Preparation of polypyrrole nanoparticles in mixed surfactants system. *Journal of Applied Polymer Science, 110*(3), 1324-1329.

Lascelles, S. F., McCarthy, G. P., Butterworth, M. D., & Armes, S. P. (1998). Effect of synthesis parameters on the particle size, composition and colloid stability of polypyrrole–silica nanocomposite particles. *Colloid & Polymer Science, 276*(10), 893-902.

Lee, J. Y., Kim, D. Y., & Kim, C. Y. (1995). Synthesis of soluble polypyrrole of the doped state in organic solvents. *Synthetic Metals, 74*(2), 103-106.

Lee, J. Y., Song, K. T., Kim, S. Y., Kim, Y. C., Kim, D. Y., & Kim, C. Y. (1997). Synthesis and Characterization of Soluble Polypyrrole. *Synthetic Metals, 84*(1-3), 137-140.

Lee, Y. H., Lee, J. Y., & Lee, D. S. (2000). A novel conducting soluble polypyrrole composite with a polymeric co-dopant. *Synthetic Metals*, *114*(3), 347-353.

Li, X.-G., Wei, F., Huang, M.-R., & Xie, Y.-B. (2007). Facile Synthesis and Intrinsic Conductivity of Novel Pyrrole Copolymer Nanoparticles with Inherent Self-Stability. *The Journal of Physical Chemistry B*, *111*(21), 5829-5836.

Liu, A. S., Bezerra, M. C., & Cho, L. Y. (2009). Electrodeposition of Polypyrrole Films on Aluminum Surfaces from a p-toluene Sulfonic Acid Medium. *Materials Research, 12*(4), 503-507.

Liu, J., & Wan, M. (2001). Synthesis, characterization and electrical properties of microtubules of polypyrrole synthesized by a template-free method. *J. Mater. Chem., 11*, 404-407.

Liu, Y., Chu, Y., & Yang, L. (2006). Adjusting the inner-structure of polypyrrole nanoparticles through microemulsion polymerization. *Materials Chemistry and Physics*, *98*(2-3), 304-308.

Omastova, M., Kosina, S., Pionteck, J., Janke, A., & Pavlinec, J. (1996). Electrical properties and stability of polypyrrole containing conducting polymer composites. *Synthetic MetaIs, 81*, 49-57.

Omastová, M., Trchová, M., Kovárová, J., & Stejskal, J. (2003). Synthesis and structural study of polypyrroles prepared in the presence of surfactants. *Synthetic Metals, 138*(3), 447-455.

Omastová, M., Trchová, M., Pionteck, J., Prokes, J., & Stejskal, J. (2004). Effect of polymerization conditions on the properties of polypyrrole prepared in the presence of sodium bis(2-ethylhexyl) sulfosuccinate. *Synthetic Metals*, *143*(2), 153-161.

Pringle, J. M., Efthimiadis, J., Howlett, P. C., Efthimiadis, J., MacFarlane, D. R., Chaplin, A. B., Hall, S. B., Officer, D. L., Wallace, G. G., & Forsyth, M. 2004. Electrochemical synthesis of polypyrrole in ionic liquids. *Polymer, 45*(5), 1447-1453.

Pyo, M., Bohn, C. C., Smela, E., Reynolds, J. R., & Brennan, A. B. (2003). Direct Strain Measurement of Polypyrrole Actuators Controlled by the Polymer/Gold Interface. *Chemistry of Materials, 15*(4), 916-922.

Ramanavicius, A., Ramanaviciene, A., & Malinauskas, A. (2006). Electrochemical sensors based on conducting polymer--polypyrrole. *Electrochimica Acta, 51*(27), 6025-6037.

Song, M.-K., Kim, Y.-T., Kim, B.-S., Kim, J., Char, K., & Rhee, H.-W. (2004). Synthesis and characterization of soluble polypyrrole doped with alkylbenzenesulfonic acids. *Synthetic Metals 141*(3), 315-319.

Thiéblemont, J. C., Gabelle, J. L., & Planche, M. F. (1994). Polypyrrole overoxidation during its chemical synthesis. *Synthetic Metals, 66*(3), 243-247.

Varela, H., Bruno, R. L., & Torresi, R. M. (2003). Ionic transport in conducting polymers/nickel tetrasulfonated phthalocyanine modified electrodes. *Polymer, 44*(18), 5369-5379.

Veeraraghavan, B., Paul, J., Haran, B., & Popov, B. (2002). Study of polypyrrole graphite composite as anode material for secondary lithium-ion batteries. *Journal of Power Sources, 109*(2), 377-387.

Wang, H., Lin, T., & Kaynak, A. (2005). Polypyrrole nanoparticles and dye absorption properties. *Synthetic Metals, 151*(2), 136-140.

Wang, L.-X., Li, X.-G., & Yang, Y.-L. (2001). Preparation, properties and applications of polypyrroles. *Reactive and Functional Polymers, 47*(2), 125-139.

Yamamoto, H., Oshima, M., Hosaka, T., & Isa, I. 1999. Solid electrolytic capacitors using an aluminum alloy electrode and conducting polymers. *Synthetic Metals*, *104*(1), 33-38.

Yan, F., Xue, G., & Zhou, M. (2000). Preparation of electrically conducting polypyrrole in oil/water microemulsion. *Journal of Applied Polymer Science, 77*(1), 135-140.

Yang, C., Liu, P., Guo, J., & Wang, Y. (2010). Polypyrrole/vermiculite nanocomposites via self-assembling and in situ chemical oxidative polymerization. *Synthetic Metals, 160*(7-8), 592-598.

Yang, C., Wang, X., Wang, Y., & Liu, P. (2012). Polypyrrole nanoparticles with high dispersion stability via chemical oxidative polymerization in presence of an anionic–non-ionic bifunctional polymeric surfactant. *Powder Technology, 217*(0), 134-139.

Zhong, W., Liu, S., Chen, X., Wang, Y., & Yang, W. (2006). High-Yield Synthesis of Superhydrophilic Polypyrrole Nanowire Networks. *Macromolecules, 39*(9), 3224-3230.